ELSEVIER

Journal of Nuclear Materials 313–316 (2003) 1178–1182

journal of nuclear materials

www.elsevier.com/locate/jnucmat

Impurity radiation during 'breathing'-like oscillations in LHD discharges using a wall limiter

B.J. Peterson [a,*], K. Sato [a], J.E. Rice [b], S. Morita [a], M. Goto [a], M. Osakabe [a], K. Tanaka [a], T. Tokuzawa [a], K. Kawahata [a], S. Masuzaki [a], S. Sakakibara [a], Y. Xu [a], A.Yu. Kostrioukov [a], N. Ashikawa [a], N. Noda [a], Y. Nakamura [a], H. Yamada [a], O. Kaneko [a], A. Komori [a], K. Yamazaki [a], S. Sudo [a], LHD Experiment Group

[a] *National Institute for Fusion Science, 322-6 Oroshi-cho, Toki-shi, Gifu 509-5292, Japan*
[b] *Plasma Science and Fusion Center, Massachusetts Institute of Technology, Cambridge, MA 02139-4294, USA*

Abstract

By changing the distribution of the coil currents in the helical coils of the large helical device (LHD) the plasma could be scraped off on the stainless steel inboard wall at the last closed flux surface, eliminating the ergodic edge region and helical divertor (HD) plasmas. During such NBI-heated discharges slow oscillations (1–2.5 Hz) have been observed in the major global parameters. These oscillations exhibit many similarities to the 'breathing' relaxation phenomenon observed during long pulse experiments in LHD when the divertor material was stainless steel. These similarities include a large core radiation fraction, significant radiation from the metallic impurities and dependence of the oscillation frequency on density. In contrast, discharges using the graphite HD show hollow radiation profiles and reduced levels of radiation from heavy impurities. Modeling shows that differences in the density dependence of the oscillation frequency between the wall limiter and HD cases can be attributed to differences in the impurity diffusion between the core and ergodic edge regions.

PACS: 52.25.Vy
Keywords: LHD; Divertor; Impurity radiation; Limiter

1. Introduction

In toroidal magnetic confinement devices the edge of the plasma is either determined by a limiter or by a magnetic divertor. In tokamaks additional field coils are used to divert the magnetic field lines from the confined volume through a *x*-point to the strike plates in the divertor region. Various divertor schemes have been useful in limiting the effect of interactions between the plasma and the wall on the core parameters [1]. Ergodic magnetic divertors have been used to spread out the heat flux and control impurities [2,3]. Recently divertors using magnetic islands have been successfully applied to W7-AS [4]. The large helical device (LHD) is unique in that it naturally has both an edge ergodic region and a continuous helical divertor (HD) [5].

The selection of divertor material is important for limiting the radiation from impurities as was seen in LHD with the reduction of metallic impurity radiation from the core immediately after replacement of the stainless steel divertor with graphite tiles [6,7]. However, radiation of heavy impurities from the core increased with time after the installation of the graphite tiles which

* Corresponding author. Tel.: +81-572 58 2239; fax: +81-572 58 2624.
E-mail address: peterson@lhd.nifs.ac.jp (B.J. Peterson).

0022-3115/03/$ - see front matter
PII: S0022-3115(02)01521-0

was attributed to deposition of stainless steel from the walls on the graphite tiles during glow discharge cleaning [8]. During long pulse discharges with a graphite HD a density window for impurity accumulation has been observed which was attributed to changes in the neoclassical transport [9]. In the presence of the stainless steel divertor in LHD a slow oscillation known as 'breathing' was observed [10] which was attributed to the repetitive influx from the divertor of sputtered metallic impurities [11]. Modeling showed that during this oscillation cooling by the light impurities at the edge could be playing an important role in turning off the sputtering and source of heavy impurities, giving the plasma a chance to recover [12,13]. Observations of changing electron and iron density profiles during the oscillation indicate that changing transport is also playing a role [14]. In this paper we describe a similar oscillation that is observed in LHD when the plasma is scraped off on the inboard wall. We compare its impurity radiation properties to those of the breathing oscillation in the case of the SS divertor and to those of a standard discharge with a graphite divertor.

2. LHD, wall limiter operation and diagnostics

LHD is a 10 field period ($l = 10$), 2 pole ($m = 2$) Heliotron device with a major radius of $R = 3.5$–3.9 m and an average minor radius of $a_c = 0.6$ m [15]. The plasmas described in this paper were heated by neutral beam injection. For the discharges described in this article the magnetic field was 1.5 T with a magnetic axis position of 3.75 for the stainless steel divertor case and 3.6 m for the other cases. The magnetic field is produced by 2 helical coils and 3 pairs of vertical field coils, all of which are superconducting. Each helical coil is divided into three separately controllable windings providing the flexibility to distort the elliptical shape of the magnetic surfaces. By adjusting the currents through these windings the shape of the plasma can be fattened in the plane of the helical coils by increasing γ ($\gamma = ma_c/lR$). The standard value of γ for LHD is 1.25 and for the wall limiter (WL) experiments described in this paper γ is increased to 1.265–1.28. This results in the divertor and ergodic region plasma being scraped off on the stainless steel (SS) inboard wall at the minor radial location, r, of the last closed flux surface $\rho = r/a_c = 1$. Due to the three dimensional shape of the vacuum vessel the plasma is scraped off at 10 locations corresponding to the toroidal angles where the vertically elongated plasma cross-section is closest to the vacuum vessel.

Vacuum ultraviolet (VUV) measurements are made using a Schwob–Fraenkel type spectrometer. Radiation profiles were obtained using two bolometer arrays (32 channels total) viewing the vertically elongated cross-section from a bottom port [16]. Inversion of the $\gamma \geqslant 1.265$ cases was made using the flux surfaces for the standard $\gamma = 1.25$ case and normalizing the edge of the plasma to $\rho = 1$. Other data shown are from standard LHD diagnostics [17].

3. Comparison of wall limiter and helical divertor plasmas

Two discharges are considered. One with a graphite HD ($\gamma = 1.25$) and the other with a SS WL ($\gamma \geqslant 1.265$). These discharges have the same heating power ($P = 2.6$ MW) and the same line averaged densities ($n_e = 2 \times 10^{19}$ m^{-3}) at the times selected. Other parameters at the selected times are shown in Table 1. Going from HD to WL cases the stored energy dropped by a factor of two while the total radiated power increased by a factor of 3.5 with corresponding increases in the radiation from light impurities. In Fig. 1 the radiation profiles for two cases are shown. Comparing the profiles one notes that while the radiation increased overall with the WL, the core increase was most dramatic. This can be attributed to the increase in the radiation from iron from the SS wall, which is seen in the VUV spectrometer data shown in Fig. 2.

4. Comparison of wall limiter oscillation with SS divertor breathing oscillation

In Fig. 3 the evolution of the global plasma parameters are shown for two discharges, one with the SS WL and one with the SS divertor. One notes that the phasings of the signals are very similar. For instance (1) the peaks in the total radiation precede the peaks in the light impurity signals and (2) begin to decay shortly after the signals from the light impurity radiation rapidly increase. This is consistent with the ideas that: (1) iron from the wall (WL case) or divertor (SS HD case) is contributing to the total radiation signal, and that (2) cooling of the edge temperature by the light impurity

Table 1

γ	n_e (10^{19} m^{-3})	W_p (kJ)	C_{III} (AU)	O_V (AU)	P_{rad} (MW)	P_{in} (MW)	P_{rad}/P_{in} (%)
1.25 (HD)	2	250	0.7	0.7	0.4	2.6	15
1.28 (WL)	2	110	2.5	3.2	1.4	2.6	55
WL/HD	1	0.4	3.5	4.6	3.5	1	3.5

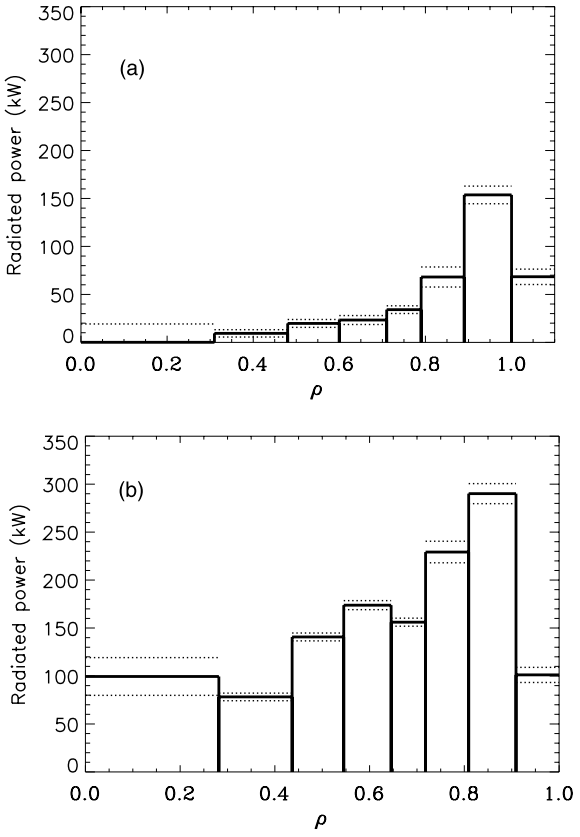

Fig. 1. Radiated power profiles for (a) graphite HD case (shot #12112 @ $t = 1.4$ s) and (b) SS WL case (shot #12090 @ $t = 1.6$ s) (in both cases $\langle n_e \rangle = 2 \times 10^{19}/m^3$). Estimated error is shown with dashed lines.

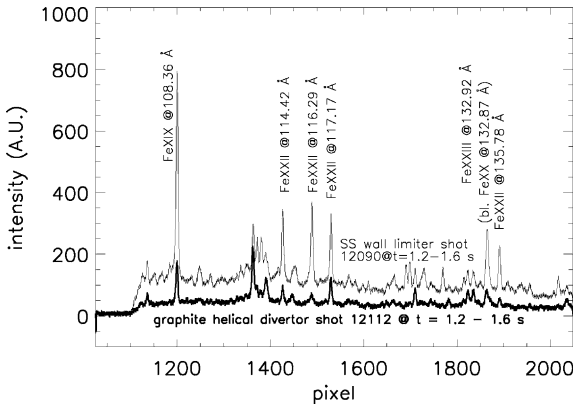

Fig. 2. Emission spectrum from VUV spectrometer for SS WL case (thin line) and graphite HD case (thick line) at the times corresponding to those of Fig. 1.

radiation reduces the divertor plasma temperature to below the sputtering threshold leading to a drop in the

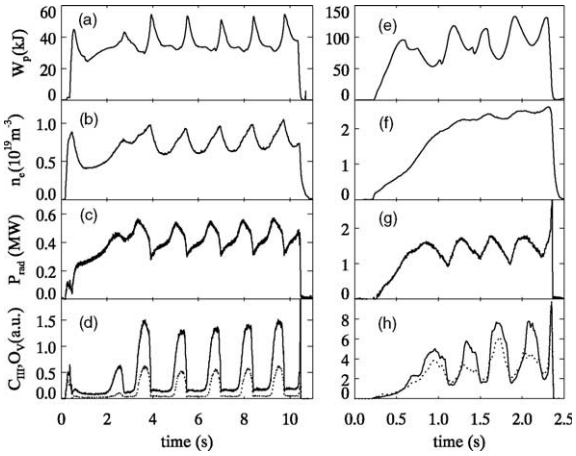

Fig. 3. Evolution of global plasma parameters for (a–d) SS helical divertor case (shot #6690) and (e–h) SS WL case (shot #12084), (a, e) stored energy, (b, f) line-averaged density, (c, g) total radiated power, (d, h) impurity radiation (O_V – solid, C_{III} – dashed).

core iron content and its associated radiation [11–13]. Both cases have similar radiation profiles at the phase where the signals from the light impurities are a minimum as seen in Fig. 4. One difference is in the much lower level of the density oscillation amplitude in the WL case. The signal shown is from a central chord while edge chords show a stronger oscillation. Another major difference is in the frequency of the oscillation. This is more clearly seen in Fig. 5 where the frequencies of the oscillations are plotted versus density. In both cases the frequencies increase with density with the WL case having a higher frequency especially at the higher densities.

5. Conclusions and discussion

In Section 3 it was seen that in the case of the WD configuration the plasma performance was seriously degraded which is attributed to the heavy influx of metallic impurities from the wall compared to the case of the graphite HD configuration. In the case of the graphite divertor low levels of radiation from iron were still observed in the VUV signals. These could be due to iron coming from the previously mentioned thin coating of stainless steel on the graphite divertor tiles [8] or due to some other source such as charge exchange neutral sputtering of the stainless steel walls.

In Section 4 we introduced a new example of a slow plasma oscillation observed in LHD with a WL configuration. Similarities in the signal phasings and the dependence of the frequency on density indicate that this belongs to the same class of oscillations observed with the SS HD known as 'breathing'. The low amplitude of

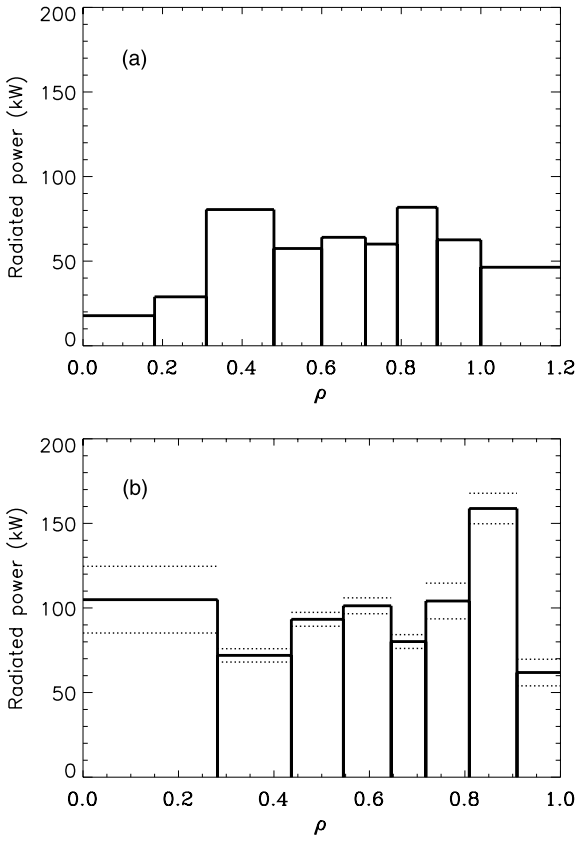

Fig. 4. Radiated power profiles for (a) SS HD case (shot #6690 @ $t = 5$ s) and (b) SS WL case (shot #12084 @ $t = 1.1$ s). Estimated error is shown with dashed lines.

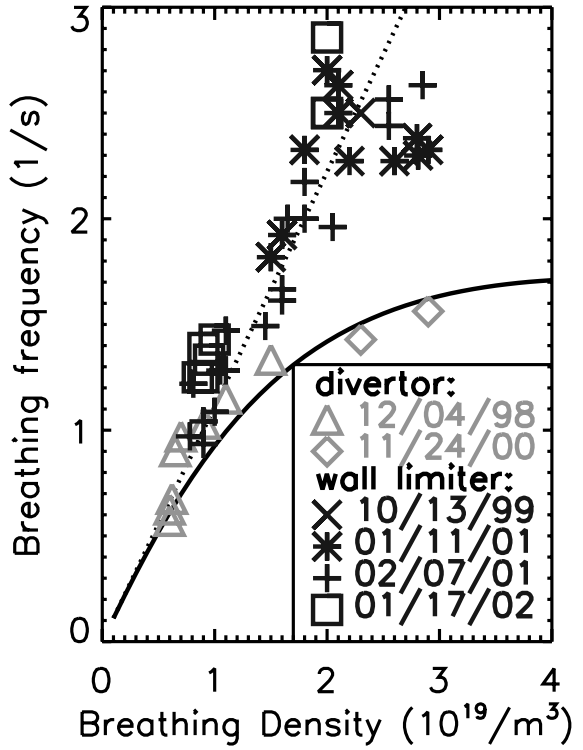

Fig. 5. Density dependence of frequency for oscillations with SS wall limiter and SS HD. Dashed line is given by Eq. (1) and solid line is given by Eq. (2).

the density oscillation in the WL case indicates that the density oscillation is not contributing significantly to the oscillation in the core radiation, which is thought to drive this phenomenon. This is consistent with the observations from the SS HD case where the core density oscillation was seen to be out of phase with the oscillation in the core radiation [11].

The observed differences in oscillation frequency dependence on density, n_e, between the HD case and the WL case in Fig. 5 can be explained in terms of a simple model of the diffusion when we assume that the oscillation is based on an impurity diffusion time, τ_I, which is related to the diffusivity, D_I, and oscillation frequency, f, as $D_I \propto f = 1/\tau_I$. In the HD case the diffusion time, τ_{HD}, is the sum of the time it takes to diffuse through the core, τ_c, and the time that it takes to diffuse through the ergodic edge region, τ_e, $\tau_{HD} = \tau_c + \tau_e$. In the WL case the ergodic edge region is scraped off and the diffusion time, τ_{WL}, is given by τ_c. The frequency of the WL case can be modeled by a linear dependence on the density,

$$f_{WL} = 1/\tau_{HD} = 1/\tau_c = 1.1 n_e(10^{-19}/m^3) \propto D_{WL} \quad (1)$$

as shown by the dashed line in Fig. 5 and as predicted by classical theory. For the HD case the data in Fig. 5 can be modeled by assuming that the edge diffusion time is given by $\tau_e = 0.18 \times \sqrt{n_e(10^{-19}/m^3)}$ and the oscillation frequency is given as

$$f_{HD} = 1/\tau_{HD} = 1/(\tau_c + \tau_e) = 1/(1/1.1 n_e + 0.18\sqrt{n_e}) \propto D_{HD} \quad (2)$$

as shown by the solid line in Fig. 5. Therefore the differences in density dependences of the oscillation frequency between the WL and HD cases as seen in Fig. 5 may be explained by a difference in the transport characteristics between the core closed field line region and the ergodic edge region. In the case of the core region a linear dependence on density is seen as predicted by classical theory. However, in the HD case the diffusion through the ergodic edge dominates at high density and according to the model used to roughly fit the data the diffusivity in the ergodic region decreases with increasing density. This indicates that density screening of impurities may be taking place in the ergodic edge region. It should be noted however, that we have not considered the role of temperature or input power, which may have some effect on the frequency scaling.

Acknowledgements

The authors would like to thank Professors M. Fujiwara and O. Motojima for their continuous support and encouragement.

References

[1] P.C. Stangeby et al., The plasma boundary of magnetic fusion devices. Institute of Physics Publishing, 2000.
[2] N. Ohyabu et al., Nucl. Fusion 25 (1985) 1684.
[3] Ph. Ghendrih et al., J. Nucl. Mater. 290–293 (2001) 798.
[4] P. Grigull et al., Plasma Phys. Control. Fusion 43 (2001) 175.
[5] N. Ohyabu et al., Nucl. Fusion 34 (1994) 387.
[6] B.J. Peterson et al., J. Nucl. Mater. 290–293 (2001) 930.
[7] S. Morita et al., Phys. Scr. T91 (2001) 48.
[8] A. Sagara et al., these Proceedings. PII: S0022-3115(02)01326-0.
[9] Y. Nakamura et al., 28th EPS CCFPP (Funchal, 2001), ECA 25A (2001) 1481.
[10] Y. Takeiri et al., Plasma Phys. Control. Fusion 42 (2000) 147.
[11] B.J. Peterson et al., Nucl. Fusion 41 (2001) 519.
[12] M.Z. Tokar et al., Phys. Plasmas 7 (2000) 4357.
[13] M.Z. Tokar et al., Contrib. Plasma Phys. 42 (2–4) (2002) 413.
[14] B.J. Peterson et al., 28th EPS CCFPP (Funchal, 2001), ECA 25A (2001) 1493.
[15] A. Komori et al., Plasma Phys. Control. Fusion 42 (2000) 1165.
[16] B.J. Peterson et al., 26th EPS CCFPP (Maastricht, 1999), ECA 23 J (1999) 1337.
[17] S. Sudo et al., Rev. Sci. Instrum. 72 (2001) 483.